Int. J. Electrochem. Sci., 7 **(2012)** 2846 - 2859

International Journal of
ELECTROCHEMICAL
SCIENCE
www.electrochemsci.org

Corrosion Passivation in Natural Seawater of Aluminum Alloy 1050 Processed by Equal-Channel-Angular-Press

El-Sayed M. Sherif[1,3,*], *Ehab A. El-Danaf*[2], *Mahmoud S. Soliman*[2], *Abdulhakim A. Almajid*[1,2]

[1]Center of Excellence for Research in Engineering Materials (CEREM), College of Engineering, King Saud University, P. O. Box 800, Al-Riyadh 11421, Saudi Arabia
[2]Department of Mechanical Engineering, College of Engineering, King Saud University, P.O. Box 800, Al-Riyadh 11421, Saudi Arabia
[3]Electrochemistry and Corrosion Laboratory, Department of Physical Chemistry, National Research Centre (NRC), Dokki, 12622 Cairo, Egypt
[*]E-mail: esherif@ksu.edu.sa

Received: 7 February 2012 / *Accepted:* 11 March 2012 / *Published:* 1 April 2012

The corrosion and corrosion passivation of aluminum alloy 1050 (AA 1050) that was fabricated by equal-channel angular press (ECAP) after different pass time numbers, namely, 0, 1, 2, and 4, in Arabian Gulf water (AGW) have been reported. The study was carried out using cyclic potentiodynamic polarization (CPP), chronoamperometric current-time (CT), and electrochemical impedance spectroscopy (EIS) measurements after 20 min and 10 days immersion in the AGW solutions. CPP experiments showed lower corrosion rate and higher corrosion resistance for the ECAPed alloy than annealed one; this effect increases with increasing the number of pass time. CT curves at –630 mV vs. Ag/AgCl and EIS spectra indicated that the increase of pass time highly decreases both uniform and pitting corrosion. Results collectively proved that the corrosion rate decreases and resistance for uniform and pitting attacks increases with increasing the number of pass time and the best performance was obtained for ECAPed AA 1050 alloy after 4 passes. For that the behavior of the cast alloy was compared to the ECAPed one after 4 passes was also reported after 10 days immersion before measurements.

Keywords: Aluminum alloy 1050; natural seawater; corrosion measurements; ECAP; electrochemical measurements

1. INTRODUCTION

The microstructure of metals can be significantly changed by subjecting the material to severe plastic deformation through procedures such as equal channel angle pressing (ECAP) and high

pressure torsion. These procedures lead to substantial grain refinement so that the grains are reduced to the submicrometer or even the nanometer range [1,2]. ECAP is a processing procedure whereby an intense plastic strain is imposed by pressing a sample in a special die. The die consists of two channels equal in cross section, intersecting at an angle ϕ, which is a subject of research in ECAP usually ranging from 90^o to 157^o [3] . There is also an additional angle Ψ, which defines the arc of curvature at the outer point of intersection of the two channels, and also it has been a subject of research. A schematic of the die can be seen in Fig. 1.

Of the various procedures that impose severe deformation, ECAP is especially the most attractive processing technique. ECAP have been utilized not only to obtain ultrafine-grained (UFG) materials but also to produce extraordinary mechanical and physical properties without remarkably changing the geometry of a bulk material. Materials processed with ECAP become superior to that of conventional coarse-grained materials [4-9]. The significant feature of ECAP is that because the billet retains the same cross-sectional area so that repetitive pressings are feasible, materials processed by ECAP may be deformed to very high strains wherein the subgrain boundaries evolve into high-angle boundaries through the absorption of dislocations, thereby producing arrays of ultrafine grains separated by high-angle grain boundaries. By contrast, this evolution cannot be achieved in more conventional metal-working processes because of the natural limit imposed on the total strain introduced during deformation [10].

Protecting aluminum from being corroded has been investigated either by adding other alloying elements and/or by decreasing the aggressiveness of its surrounding corrosive environments. Decreasing the corrosivity of the environments can be done mostly by using corrosion inhibitors [11-17] or protective coatings [18, 19]. The inhibition of the alloy surface is usually obtained by inorganic oxidants such as chromate, molybdate, and tungstate [20-23] or organic compounds having polar groups, such as oxygen, sulfur and nitrogen as well as heterocyclic compounds containing functional groups and conjugated double bonds [11-17]. ECAP is considered as one of the very useful methods for producing ultra-fine microstructures of Al-based alloys with significantly improved mechanical properties and higher corrosion resistance [24-26]. In addition, some ultra-fine grained Al-based alloys produced by ECAP showed a superplastic forming capability [27, 28].

The objective of this work was to study the effect of ECAP pass time number that varied from 1 to 4 on the corrosion of the annealed aluminum alloy 1050 (AA 1050) in Arabian Gulf water. A particular attention was paid to the effect of pass time number on the pitting corrosion of the AA 1050. The study was achieved by using different electrochemical techniques such as cyclic potentiodynamic polarization, chronoamperometric current-time variations, and electrochemical impedance spectroscopy.

2. EXPERIMENTAL PROCEDURE

2.1. Fabrication of the ECAPed AA 1050

The die, Fig. 1, was manufactured from hot work tool steel. The die angles were designed and manufactured to have: Ψ=0 and ϕ=90^o. Route B_C, where the sample was rotated by 90^o between

subsequent pressings was adopted in the present study. Commercial purity aluminum (AA 1050) containing the following impurities, Fe–0.40% min, Si–0.25%, Cu–0.05%, Mn–0.05%, Mg–0.05%, Cr–0.05%, Zn–0.05%, V–0.05%, Ti–0.03%, others 0.03% and Al–balance) with purity of 99.5% was used in this study. The material was supplied as cold rolled plates of 15 mm thickness. Cylindrical samples were machined parallel to the rolling direction, and then annealed at a temperature of 600 ^{o}C for 8 hours, to give an average grain size of about 600μm. The annealed samples were lubricated using graphite based lubricant and pressed in the ECAP die. The Vickers microhardness (kg/mm^2) was measured using a Buehler micromet hardness tester at a load of 300 g and the reported value is the average of 20 readings. Samples of about 6 mm in length were cut from the ECAP processed samples and pressed in a direction parallel to the extrusion direction to document the yield strength.

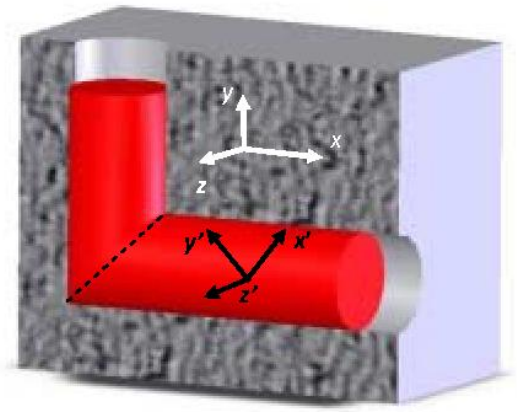

Figure 1. Schematic representation of the ECAP process showing the billet axes system *xyz* and the reference shear axis system *x'y'z'*.

2.2. Corrosion tests

2.2.1. Chemicals and electrochemical cell

The natural sea water was brought from the Arabian Gulf at the eastern region (Jubail, Dammam, Saudi Arabia) and was used as received. An electrochemical cell with a three-electrode configuration was used for electrochemical measurements. Annealed and ECAPed AA 1050 rods were used in this study. The AA 1050 rod, a platinum foil, and a Metrohm Ag/AgCl electrode (in 3 M KCl) were used as working, counter, and reference electrodes, respectively.

The AA 1050 rods for electrochemical measurements were prepared by welding a copper wire to a drilled hole was made on one face of the rod; the rod with the attached wire were then cold mounted in resin and left to dry in air for 24 h at room temperature. Before measurements, the other face of the Al electrode, which was not drilled, was grinded successively with metallographic emery paper of increasing fineness of up to 800 grits. The electrodes were then washed with doubly distilled water, degreased with acetone, washed using doubly distilled water again and finally dried with tissue paper. In order to prevent the possibility of crevice corrosion during measurement, the interface

between sample and resin was coated with Bostik Quickset, a polyacrelate resin. The total exposed surface area of the working electrode was 1.0 cm^2.

2.2.2. Electrochemical methods

Electrochemical experiments were performed by using an Autolab Potentiostat (PGSTAT20 computer controlled) operated by the general purpose electrochemical software (GPES) version 4.9. The CPP curves were obtained by scanning the potential in the forward direction from -1800 to -500 mV against Ag/AgCl at a scan rate of 3.0mV/s; the potential was then reversed in the backward direction. Chronoamperometric current-time experiments were carried out by stepping the potential of the AA 1050 rods at – 630 mV versus Ag/AgCl; in some experiments this potential value was applied after stepping the potential of Al to -1000mV vs. Ag/AgCl for 20 min. EIS tests were performed at corrosion potentials (E_{Corr}) over a frequency range of 100 kHz – 100 mHz, with an ac wave of ± 5 mV peak-to-peak overlaid on a dc bias potential, and the impedance data were collected using Powersine software at a rate of 10 points per decade change in frequency. ZSimpWin software was used to fit the EIS data to best equivalent circuit for Al rods in AGW. All the electrochemical experiments were recorded after the electrode immersion in the test solution for 20 min and in some cases the electrodes were immersed for 10 days before measurements. All measurements were also carried out at room temperature in freely aerated stagnant solutions.

3. RESULTS AND DISCUSSION

3.1. Cyclic potentiodynamic polarization (CPP) data

In order to study the effect of the number of ECAP pass time on the corrosion behavior of AA 1050 in AGW solution, CPP experiments were carried out. The CPP curves for (1) 0 pass, (2) 1 pass, (3) 2 passes, and (4) 4 passes ECAPed AA 1050, respectively after 20 min immersion in AGW solutions are shown in Fig. 2. It has been reported [12, 13] that the cathodic reaction for Al in aerated near neutral pH solutions is the oxygen reduction followed by its adsorption i.e.

$$O_2 + 2H_2O + 4e^- = 4OH^- \quad (1)$$

The presence of oxygen enhances the cathodic reaction due to oxygen reduction and transforms aluminum to aluminum hydroxide as follows,

$$Al_{(S)} + 3OH^- = Al(OH)_{3,ads.} + 3e^- \quad (2)$$

The aluminum hydroxide, $Al(OH)_3$, is transformed to $Al_2O_3.3H_2O$,

$$2Al(OH)_{3,ads.} = Al_2O_3.3H_2O \quad (3)$$

The formed Al_2O_3 is of a dual nature and consists of an adherent, compact, and stable inner oxide film covered with a porous, less stable outer layer, which is more susceptible to corrosion [21, 29, 30].

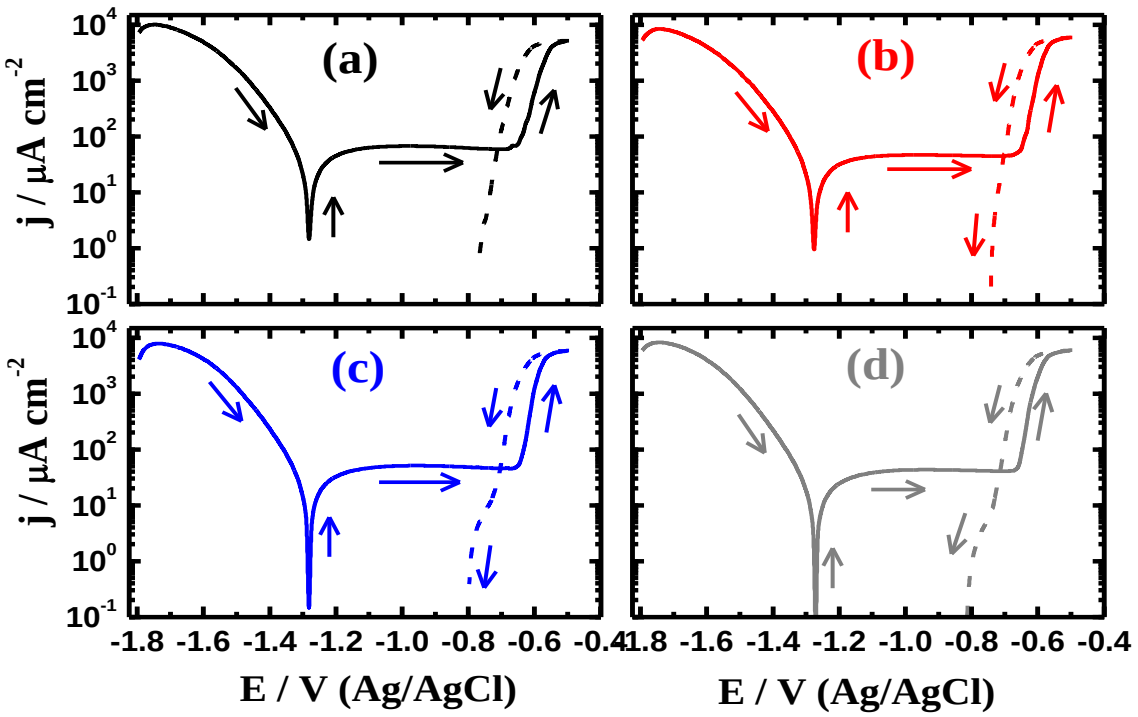

Figure 2. CPP curves obtained for (a) annealed, (b) 1 pass, (c) 2 passes, and (d) 4 passes ECAPed AA 1050 electrode, respectively after its immersion in AGW for 20 minutes.

It is clearly seen from Fig. 2, curve 1, that the anodic reaction of Al started from the corrosion potential (–1285 mV vs. Ag/AgCl) towards the less negative potential values to show a passive region at an average current density of 62.2 μA/cm^2, extending from −1150 to −680 mV. In this potential range, aluminum oxide is formed on the surface according to reaction (3). After which the current shows an abrupt increase in its values with increasing the applied potential due to the breakdown of the formed oxide film and the occurrence of pitting corrosion, accordingly the dissolution of aluminum can be expressed by the reaction [11-13, 31, 32];

$$Al = Al^{3+}. + 3e^- \quad (4)$$

This occurs under the influence of the attack of the aggressive chloride ions that present in the seawater to the aluminum in the flawed areas of the oxide film, which leads to the formation of the soluble aluminum chloride complex;

$$Al^{3+} + 4Cl^{-} = AlCl_4^{-} \quad (5)$$

Here, there are two points of views explaining the mechanism of pitting corrosion at this condition. The first claims [32, 33] that a salt barrier of $AlCl_3$ is formed within the pits on their formation, which could lead to the formation of $AlCl_4^{-}$ as repersented by Eq. 5, and diffuses into the bulk of the solution. While, the second [34] has proposed that the chloride ions do not enter into the oxide film but they are chemisorbed onto the oxide surface and act as a reaction partner, aiding the oxide to dissolve via the formation of oxy-chloride complexes as follows:

$$Al^{3+}_{(\text{in crystal lattice of the oxide})} + 2Cl^{-} + 2OH^{-} = Al(OH)_2Cl_2^{-} \quad (6)$$

The occurrence of pitting corrosion was also indicated by the appearance of the hysteresis loop on reversing the potential scan in the backward direction towards the more negative values. This loop appeared due to higher current values in the reverse scan than the forward values. The bigger the area of the loop the more severe is the pitting corrosion.

The CPP curves of ECAPed alloy show almost similar behavior but with lower corrosion rates and higher corrosion resistances. This was indicating by recording the values of the corrosion potential (E_{Corr}), corrosion current (j_{Corr}), cathodic (βc) and anodic Tafel slopes (βa), passivation current (j_{Pass}), protection potential (E_{Prot}), pitting potential (E_{Pit}), polarization resistance (R_P), and corrosion rate (K_{Corr}), obtained from CPP curves (Fig. 2) for the annealed and ECAPed AA 1050 alloys after their immersion in AGW solutions for 20 min and shown in Table 1. The values of the corrosion potential and corrosion current were obtained from the extrapolation of anodic and cathodic Tafel lines located next to the linearized current regions. The pitting potential was determined from the forward anodic polarization curves where a stable increase in the current density occurs. The protection potential was determined from the backward anodic polarization curve at the intersection point with the forward polarization curve. The values of R_P and K_{Corr} were calculated from the polarization data as reported in our previous work [35-44].

It is seen from Fig. 2 and Table 1 that the AA 1050 alloy pressed by ECAP shifted the values of E_{Corr} to less negative values, lowered the values of j_{Corr}, $j_{Pass,}$ and K_{Corr}, and increased the values of R_P. This effect is significantly increased with increasing the number of pass time to reach its maximum after 4 passes. For that CPP behavior of the annealed AA 1050 alloy was compared to the fabricated alloy by ECAPed for 4 passes after 10 days immersion in sea water before measurements as repersented by Fig. 3a and Fig. 3b, respectively. The corrosion parameters obtained from Fig. 3 are shown in Table 1. Fig. 3 and Table 1 show that the ECAPed alloy recorded lower corrosion rate and higher corrosion resistance than the annealed alloy and both of the alloys showed better performance compared to their CPP behavior when the immersion time was only 20 min. This indicates that the increase of immersion time decreases the corrosion of annealed and ECAPed AA 1050 alloys. According to Chung et al. [6] the increase of ECAP pass number increases the corrosion resistance of AA 1050 due to the decreasing of the size of the Si-containing impurities on the alloy surface. Where, the presence of these Si-containing impurities induced the micro-galvanic reaction by its reaction with the Al matrix and also between the Al matrix and the Si-containing oxide.

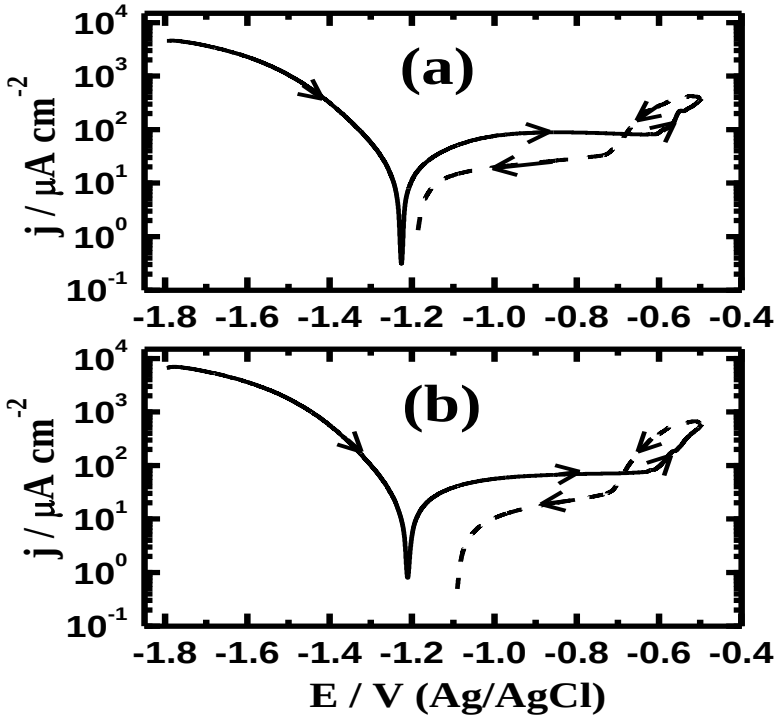

Figure 3. CPP curves obtained for (a) annealed and (b) 4 passes ECAPed AA 1050 electrode after its immersion in AGW for 10 days before measurement.

Table 1. Corrosion parameters obtained from polarization curves shown in Fig. 2 and Fig. 3 for AA 1050 after 20 min and 10 days of the electrode immersion in Arabian Gulf water.

AA 1050 alloy	Parameter								
	β_c / mV dec^{-1}	E_{Corr}/ mV	j_{Corr}/ μAcm^{-2}	β_a/ mV dec^{-1}	j_{Pass}/ μAcm^{-2}	E_{Prot}/ mV	E_{Pit}/ mV	R_p/ Ωcm^2	K_{Corr}/ mmy^{-1}
0 pass (20 min)	100	-1285	27	110	62.2	-720	-655	0.84	0.294
1 pass (20 min)	105	-1270	22	115	50.0	-710	-645	1.10	0.240
2 pass (20 min)	110	-1260	18	120	49.9	-705	-643	1.37	0.196
4 pass (20 min)	110	-1255	15	125	42.1	-710	-640	1.70	0.164
0 pass (10 days)	135	-1225	19	153	89.7	-680	-610	1.64	0.207
4 pass (10 days)	140	-1210	13	155	61.6	-680	-620	2.46	0.142

3.2. Chronoamperometric current-time (CT) measurements

In order to shed more light on the effect of ECAP pass time on the pitting corrosion of Al AA 1050 after 20 min and 10 days immersion in AGW at more anodic constant potential value, chronoamperometric experiments were carried out. Fig. 4 represents the variation of the measured dissolution currents versus time at –630 mV vs. Ag/AgCl for the annealed (1) and ECAPed (2) 1 pass, (3) 2 passes, and (4) 4 passes AA 1050 alloy, respectively after 20 min immersion in AGW. The same experiments were conducted on the different Al rods after applying –1000 mV (this potential was chosen from the CPP curves, where it allows the alloy to develop a compact passive layer) for 10 min

before stepping the potential to –630 mV and the curves are shown in Fig. 5. It is seen from Fig. 4 that the highest current values were recorded for the annealed alloy (curve 1), where the current increased upon applying the potential in the first hundreds of seconds, the current then decreased slightly with time for the whole time of the experiment. For the ECAPed alloys, the current-time curves showed the same behavior with lower absolute currents. This effect increases with increasing the pass time number, where the ECAPed alloy fabricated at 4 passes showed the lowest absolute current with time. This behavior indicates that the increase of pass time number to 4 passes decreased the uniform corrosion of AA 1050 in AGW.

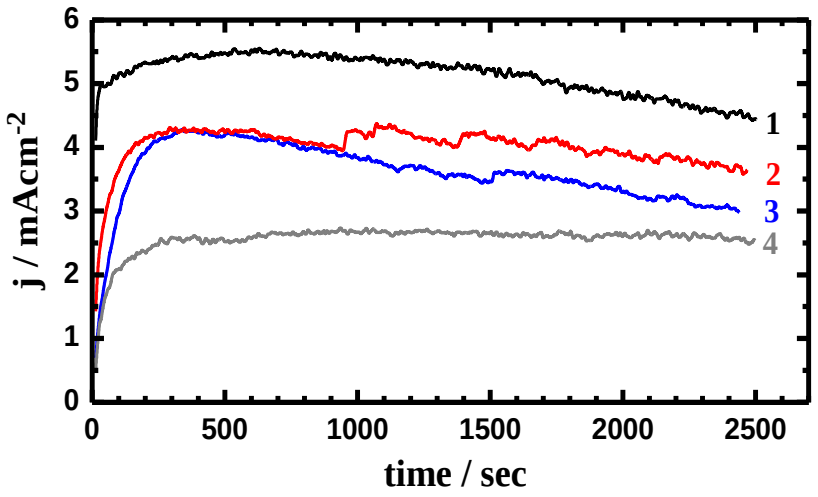

Figure 4. Chronoamperometric curves obtained for (1) annealed, (2) 1 pass, (3) 2 passes, and (4) 4 passes ECAPed AA 1050 electrode after its immersion in AGW solutions for 20 minutes followed by stepping the potential to –630mV vs. Ag/AgCl.

The current-time curves depicted in Fig. 5 showed similar behavior to those shown in Fig. 4 at the same potential, with possible occurrence of pitting corrosion due to the attack of the aggressive ions present in the AGW to the flawed area of the passive layer that was formed at –1000 mV. From the chronoamperometric experiments the annealed alloy showed the worst corrosion resistance, while the best performance was recorded for the ECAPed alloy after 4 passes, for that the CT curves at –630 mV for (1) annealed and (2) 4 passes ECAPed AA 1050, respectively after 10 days immersion in the AGW were carried out as shown in Fig. 6. The current for annealed alloy recorded very low values at the few seconds of the measurement due to the formed corrosion products and oxide layer on the surface during the 10 days immersion. The current then started to increase rapidly accompanied by large fluctuations, which indicate on the occurrence of severe pitting corrosion. On the other hand, the current for the ECAPed alloy recorded very low current values (few microamperes) for the whole time of the experiment, which indicate that the formed passive layer during the immersion time was compact enough to protect the surface from being pitted and attacked by the corrosive species that present in the Gulf water at the applied potential. This also agrees with the work reported by Chung et al. [6] that the increase of ECAP pass time number increases the pitting resistance of the alloy.

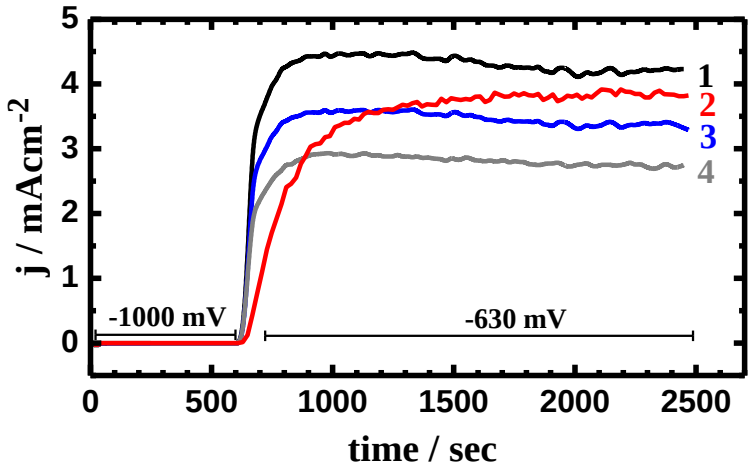

Figure 5. Chronoamperometric curves obtained for (1) annealed and (2) 1 pass, (3) 2 passes, and (4) 4 passes ECAPed AA 1050 electrodes after their immersion in AGW solutions for 20 min followed by stepping the potential to –1000 mV for 10 minutes and finally fix it to –630mV vs. Ag/AgCl.

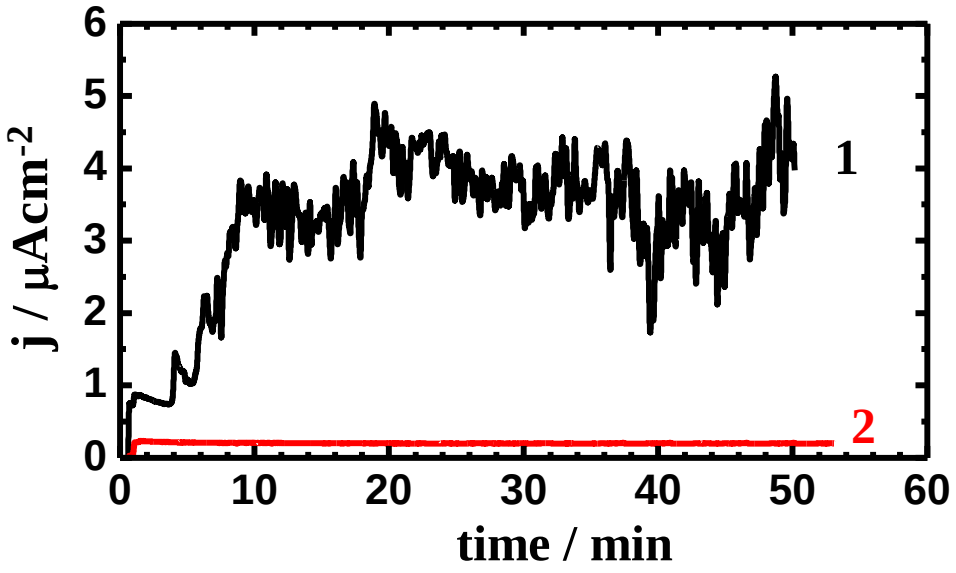

Figure 6. Chronoamperometric curves obtained for (1) annealed and (2) 4 passes ECAPed AA 1050 rods after their immersion in AGW for 10 days before stepping the potential to –630mV vs. Ag/AgCl.

3.3. Electrochemical impedance spectroscopy (EIS) measurements

The EIS has successfully employed to explain the corrosion and corrosion inhibition of several metals and alloys in chloride media [45-55]. The method was used to determine kinetic parameters for electron transfer reactions at the alloy/electrolyte interface. The EIS Nyquist plots obtained for (1) annealed, (2) ECAPed 1 pass, (3) ECAPed 2 passes, and (4) ECAPed 4 passes AA 1050 alloy, respectively after 20 min immersion in AGW are shown in Fig. 7. The Nyquist (a), Bode (b) and phase

angle (c) plots for (1) annealed and (2) ECAPed 4 passes AA 1050 alloy, respectively after 10 days are also shown in Fig. 8. The EIS data of the Nyquist spectra shown in Fig. 7 and Fig. 8a were analysed by fitting to the equivalent circuit model shown in Fig. 9. The parameters obtained by fitting the equivalent circuit are listed in Table 2. Here, R_S represents the solution resistance between the alloy surface and the counter (platinum) electrode, Q the constant phase elements (CPEs) and contain two parameters; a pseudo capacitance and an exponent (an exponent of less than unity indicates a dispersion of capacitor effects [12, 13]), the R_{P1} accounts for the resistance of a film layer formed on the alloy surface, C_{dl} is the double layer capacitance, C_{dl} is the double layer capacitance, and R_{P2} accounts for the charge transfer resistance at the alloy surface, i.e. the polarization resistance.

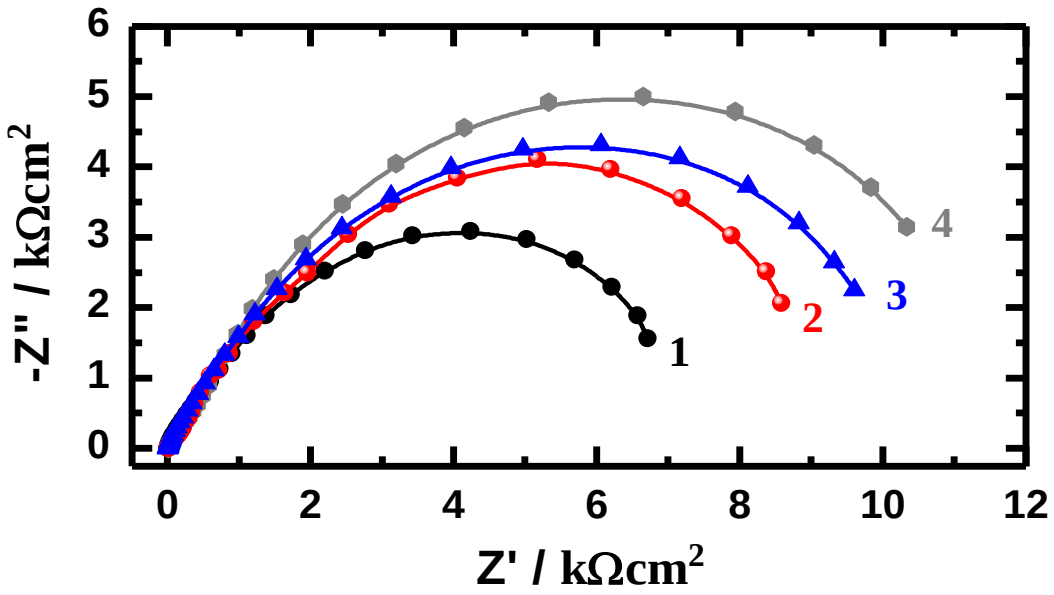

Figure 7. Nyquist plots obtained for (1) annealed, (2) 1 pass, (3) 2 passes, and (4) 4 passes ECAPed AA 1050 electrode at an open circuit potential after its immersion in AGW for 20 min.

Nyquist spectra shown in Fig. 7 and Fig. 8a with the parameters recorded in Table 2 clearly revealed that the values of R_S, R_{P1} and R_{P2} increased with increasing the pass time number for the AA 1050 alloy. This is attributed to the formation of a passive film and/or corrosion products, which gets thicker with time and could lead to the decrease in j_{Corr} and K_{Corr} and also the increase in R_P values we have seen in polarization data (Fig. 2, Fig. 3 and Table 1) under the same conditions. The semicircles at high frequencies in Fig. 7 and Fig. 8a are generally associated with the relaxation of electrical double layer capacitors and the diameters of the high frequency semicircles can be considered as the charge transfer resistance ($R_P = R_{P1} + R_{P2}$) [37].

The polarization resistance measured by EIS is a measure of the uniform corrosion rate as opposed to tendency towards localized corrosion. The decrease C_{dl} values with ECAP pass time is due to the reduced access of charged species to the surface suggest that the dissolution of the alloy via mass transport decreases. The CPEs (Q) with their n values > 0.5 and close to 1.0 represent double

layer capacitors with some pores; the decrease of CPEs with the increase of number of ECAP passes provides another indication on the increased passivation of AA 1050.

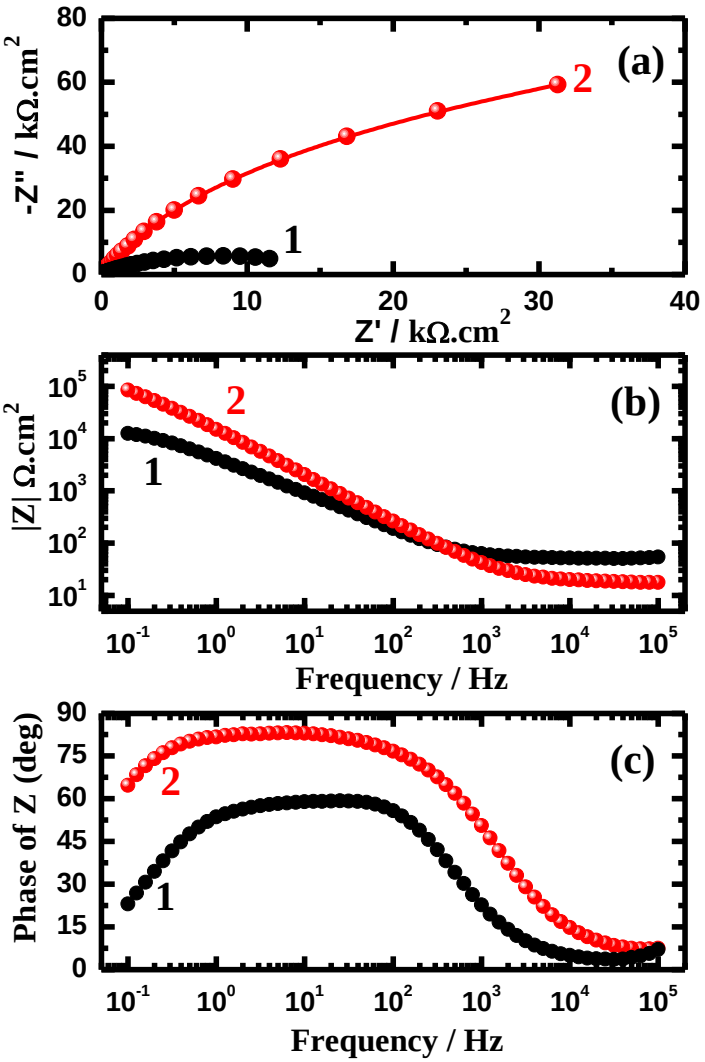

Figure 8. Nyquist (a), Bode (b) and phase angle (c) plots for (1) annealed alloy and (2) 4 passes ECAPed AA 1050 electrode at an open circuit potential after its immersion in AGW for 10 days.

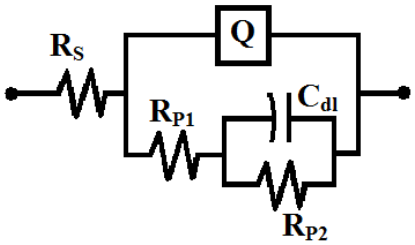

Figure 9. The equivalent circuit model used to fit the experimental data presented in Fig. 7 and Fig. 8a. See text for symbols used in the circuit.

Table 2. EIS parameters obtained by fitting the Nyquist plots shown in Fig. 7 and Fig. 8a with the equivalent circuit shown in Fig. 9 for AA 1050 electrodes after 20 min and 10 days of immersion in Arabian Gulf water.

AA 1050 alloy	Parameter					
	R_S / Ω cm^2	Q		R_{P1} / k Ω cm^2	C_{dl} / μF cm^{-2}	R_{P2} / k Ω cm^2
		Y_Q/ μF cm^{-2}	n			
0 pass (20 min)	6.23	32.89	0.83	0.201	26.14	5.51
1 pass (20 min)	8.81	25.34	0.80	0.860	19.01	7.75
2 passes (20 min)	9.45	14.30	0.80	2.86	16.75	9.19
4 passes (20 min)	11.28	5.48	0.76	1.731	13.07	11.39
0 pass (10 days)	8.90	0.56	0.80	1.91	2.79	9.58
4 passes (10 days)	12.49	0.19	0.88	3.28	1.89	23.98

Increasing the immersion time from 20 min to 10 days also enhances the values of R_S, R_{P1}, and R_{P2} and decreases the values of CPEs and C_{dl}, which means the alloy surface gets more passivated as the exposure time before measurements increases. Elongation of immersion period leads to accumulation of corrosion products and protective oxide layers on the alloy surface and thus decreases the uniform corrosion. This was also confirmed by the increase in the impedance of the interface (Fig. 8b) and the maximum phase angle (Fig. 8c) with increasing the immersion time. In general, EIS results agree with CPP and CT measurements that the corrosion AA 1050 decreases with increasing the ECAP pass time number as well as the immersion time of the alloy in the test solution before measurement.

4. CONCLUSIONS

A series of aluminum alloy 1050 was fabricated by using ECAP process after 0, 1, 2, and 4 passes. The electrochemical behavior of the annealed and the ECAPed AA 1050 in Arabian Gulf water was investigated using variety of electrochemical methods. Cyclic polarization tests after 20 min and 10 days immersion in AGW indicated that the increase of ECAP passes time as well as immersion time decrease the uniform corrosion of the alloy. The variation of current against time at – 630 mV vs. Ag/AgCl after 20 min and 10 days also revealed that the dissolution of AA 1050 decreased with increasing the pass time number, while increasing the exposure time increases the pitting corrosion of the annealed alloy. Electrochemical impedance spectra proved that the solution and polarization resistances decreased with increasing the pass time number up to 4 and immersion intervals. The results together were internally consistent with each other, indicating clearly that the dissolution of the alloy decreased with increasing the number of ECAP pass time and the best performance was shown by 4 passes ECAPed AA 1050 and this effect increased with increasing the immersion time from 20 minutes to 10 days.

ACKNOWLEDGEMENT
The authors are grateful to the Center of Excellence for Research in Engineering Materials (CEREM) for the financial support.

References

1. Cheng Xu, S.V. Dobatkin, Z. Horita, T.G. Langdon, *Mater. Sci. Eng. A*, 500 (2009) 170–175.
2. Ehab A. El-Danaf, *Mater. Sci. Eng. A,* 487 (2008) 189–200.
3. K. Nakashima, Z. Horita, M. Nemoto, T.G. Langdon, *Acta Mater.,* 46 (1998) 1589–99.
4. S. Rusz, K. Malaník, J. Kedroň, Arch. Mater. Sci. Eng., 34 (2008) 52–56.
5. Jiang Jing-hua, Ma Ai-bin, Song Dan, N. Saito, Yuan Yu-chun, Y. Nishida, *Trans. Nonferrous Met. Soc. China,* 20 (2010) 195–200.
6. Min-Kyong Chung, Yoon-Seok Choi, Jung-Gu Kim, Young-Man Kim, Jae-Chul Lee, *Mater. Sci. Eng. A,* 366 (2004) 282–291.
7. Zhang Jing, Zhang Ke-shi, Wu Hwai-Chung, YU Mei-hua, *Trans. Nonferrous Met. Soc. China,* 19 (2009) 1303–1311.
8. A. Vinogradov, A. Washikita, K. Kitagawa, V.I. Kopylov, *Mater. Sci. Eng. A,* 349 (2003) 218–326.
9. Dan Song, AiBin Ma, Jinghua Jiang, Pinghua Lin, Donghui Yang, Junfeng Fan, *Corros. Sci.,* 52 (2010) 481–490.
10. R.Z. Valiev, T.G. Langdon, *Prog. Mater. Sci.,* 51 (2006) 881–981.
11. El-Sayed M. Sherif, *Int. J. Electrochem. Sci.,* 6 (2011) 1479.
12. E.M. Sherif, S.-M. Park, *Electrochim. Acta,* 51 (2006) 1313.
13. E.M. Sherif, S.-M. Park, *J. Electrochem. Soc.,* 152 (2005) B205.
14. N.A. Ogurtsov, A.A. Pud, P. Kamarchik, G.S. Shapoval, *Synth. Met.*, 143 (2004) 43.
15. I.B. Obot1, N.O. Obi-Egbedi, *Int. J. Electrochem. Sci.,* 4 (2009) 1277.
16. A.Y. El-Etre, *Corros. Sci*., 43 (2001) 1031.
17. S.B. Saidman, J.B. Bessone, *J. Electroanal. Chem.,* 521 (2002) 87.
18. R. Zandi-zand, A. Ershad-langroudi, A. Rahimi, *J. Non-Crystalline Solids,* 351 (2005) 1307–1311.
19. J.M. Vega, N. Granizo, D. de la Fuente, J. Simancas, M. Morcillo, Prog. Org. Coat. 70 (2011) 213.
20. P.M. Natishan, E. McCafferty, G.K. Hubler, *J. Electrochem. Soc.,* 135 (1988) 321.
21. C.M.A. Brett, I.A.R. Gomes, J.P.S. Martins, *Corros. Sci.,* 36 (1994) 915.
22. S.S.A. Rehim, H.H. Hassan, M.A. Amin, *Appl. Surf. Sci.,* 187 (2002) 279.
23. S. Zein El Abedin, *J. Appl. Electrochem.,* 31 (2001) 711.
24. M. Fujda, T. Kvačkaj, K. Nagyová, *J. Met. Mater. Miner.,* 18 (2008) 81–87.
25. Eiji Akiyama, Zuogui Zhang, Yoshimi Watanabe, Kaneaki Tsuzaki, *J. Solid State Electrochem.,* 13 (2009) 277–282.
26. M. Furukawa, Z. Horita, M. Nemoto, T.G. Langdon, *J. Mater. Sci*. 36 (2001) 2835 – 2843.
27. M. Furukawa, Z. Horita, T. G. Langdon, *Adv. Eng. Mater.,* 3 (2001) 121 – 125.
28. Z. Horita, S. Lee, S. Ota, K. Neishi, T.G. Langdon, *Mater. Sci. Forum.* 357–359 (2001) 471–476.
29. G.Y. Elewady, I.A. El-Said, A.S. Fouda, *Int. J. Electrochem. Sci.,* 3 (2008) 177.
30. F.D. Wall, M.A. Martinez, J.J. Vandenavyle, *J. Electrochem. Soc.,* 151 (2004) B354.
31. El-Sayed M. Sherif, A.A. Almajid, F.H. Latif, H. Junaedi, *Int. J. Electrochem. Sci.,* 6 (2011) 1085-1099.
32. F.H. Latief, El-Sayed M. Sherif, A.A. Almajid, H. Junaedi, *J. Anal. Appl. Pyrol.,* 92 (2011) 485-492.
33. F. Hunkeler, G.S. Frankel, H. Bohni, *Corrosion (Houston),* 43 (1987) 189.
34. L. Tomcsanyi, K. Varga, I. Bartik, G. Horanyi, E. Maleczki, *Electrochim. Acta,* 34 (1989) 855.
35. E.M. Sherif, S.-M. Park, *Corros. Sci.,* 48 (2006) 4065.
36. E.M. Sherif, S.-M. Park, *J. Electrochem. Soc.,* 152 (2005) B428.
37. E.M. Sherif, S.-M. Park, *Electrochim. Acta,* 51 (2006) 6556.
38. El-Sayed M. Sherif, J.H. Potgieter, J.D. Comins, L. Cornish, P.A. Olubambi, C.N. Machio, *J. Appl. Electrochem.,* 39 (2009) 1385.

39. El-Sayed M. Sherif, J.H. Potgieter, J.D. Comins, L. Cornish, P.A. Olubambi, C.N. Machio, *Corros. Sci.*, 51 (2009) 1364.
40. El-Sayed M. Sherif, A.A. Almajid, *J. Appl. Electrochem.*, 40 (2010) 1555.
41. El-Sayed M. Sherif, R.M. Erasmus, J.D. Comins, *J. Electrochim. Acta*, 55 (2010) 3657.
42. El-Sayed M. Sherif, R.M. Erasmus, J.D. Comins, *J. Appl. Electrochem.*, 39 (2009) 83.
43. El-Sayed M. Sherif, R.M. Erasmus, J.D. Comins, *Corros. Sci.*, 50 (2008) 3439.
44. El-Sayed M. Sherif, R.M. Erasmus, J.D. Comins, *J. Colloid Inter. Sci.*, 209 (2007) 470.
45. El-Sayed M. Sherif, A.A. Almajid, *Int. J. Electrochem. Sci.*, 6 (2011) 2131-2148.
46. E.M. Sherif, S.-M. Park, *J. Electrochim. Acta*, 51 (2006) 4665.
47. El-Sayed M. Sherif, R.M. Erasmus, J.D. Comins, *J. Colloid Interface Sci.*, 306 (2007) 96.
48. El-Sayed M. Sherif, R.M. Erasmus, J.D. Comins, *J. Colloid Interface Sci.*, 311 (2007) 144.
49. El-Sayed M. Sherif, *Int. J. Electrochem. Sci.*, 6 (2011) 2284-2298.
50. El-Sayed M. Sherif, *Mater. Chem. Phys.*, 129 (2011) 961-967.
51. El-Sayed M. Sherif, *Int. J. Electrochem. Sci.*, 6 (2011) 2077-3092.
52. El-Sayed M. Sherif, A.A. Almajid, A.K. Bairamov, Eissa Al-Zahrani, *Int. J. Electrochem. Sci.*, 6 (2011) 5430-5444.
53. El-Sayed M. Sherif, *Int. J. Electrochem. Sci.*, 6 (2011) 5372-5387.
54. Khalil A. Khalil, El-Sayed M. Sherif, A.A. Almajid, *Int. J. Electrochem. Sci.*, 6 (2011) 6184-6199.
55. El-Sayed M. Sherif, *Int. J. Electrochem. Sci.*, 7 (2012) 1482-1495.